DOI 10.17816/transsyst20184390-101

© M. Kato, K. Hirata
Osaka University
(Osaka, Japan)

CONTROL OF THREE-DEGREE-OF-FREEDOM RESONANT ACTUATOR DRIVEN BY NOVEL VECTOR CONTROL

Abstract. This paper presents a novel vector control method for three-degree-of-freedom resonant actuator in order to improve its controllability. The effectiveness of the presented method is verified through electromagnetic field analysis using 3-D finite element method:

Issue: A three-degree-of-freedom resonant actuator has a great potential to broaden the application range of linear oscillatory actuators because it has a lot of advantages: high efficiency, simple structure, etc. However, this actuator has low controllability because the magnetic structure of each axis is not independent.

Aim: To establish a novel vector control technique suitable for our actuator.

Methods: Electromagnetic analysis employing 3-D finite element method.

Results: In this study, the novel vector control theory was constructed on the basis of four-phase system. The new dq model was achieved by considering 3-D coordinate transformation. The proposed method is able to decrease the influence of thrust interference from other axis and achieved higher controllability.

Conclusion: The results of the study will contribute to a practical use of the three-DOF resonant actuator.

Keywords: linear actuators, linear oscillaory actuators, vector control, multi degree-of-freedom actuators, finite element analysis, four-phase system, dq tranformation.

INTRODUCTION

Linear resonant actuators (LRAs) [1–5] have been used in a wide range of applications because they can reciprocate in a comparatively short stroke in spite of their compact size and lightweight. In order to broaden the application range of LRAs, various kinds of multi-degree of freedom (DOF) resonant actuators have been developed [6, 7]. Authors have also proposed a two degree-of-freedom resonant actuator that was able to be independently driven in x- and z-axes by vector control [8–10]. Additionally, authors have designed a three-DOF resonant actuator driven by conventional vector control [11]. However, the previous control method did not completely control the thrusts in three directions (x, y, and z) because the magnetic circuit for each axis was not independent.

Received: 30.06.2018. Revised: 30.06.2018. Accepted: 01.10.2018.

In order to improve controllability of the thrust, this paper proposes a novel vector control method using a four-phase system. Four fundamental voltage vectors (V_x, W_x, V_y, and W_y phases) are defined in a stationary three-dimensional (3-D) coordinate systems. 3-D rotation using Euler angles achieved a spatial dq transformation. Electromagnetic field analysis by 3-D finite element method suggested that *x*- and *y*-axes thrust did not affect each other strongly when the proposed vector control was applied. Finally, the effectiveness of the proposed method was validated by comparing with the conventional method.

THREE-DOF RESONANT ACTUATOR AND OPERATING PRINCIPLE

The basic structure of the three-DOF resonant actuator is shown in Fig. 1. This actuator mainly consists of a mover, a stator, and resonance springs in the *x*-, *y*-, and *z*-directions that support the mover. The mover is composed of a cross-shaped laminated yoke with five excitation coils (45 turns). This actuator is assumed to move with a range of ±1.2mm in the *x*-and *y*-directions and ±0.5mm in the *z*-direction, respectively. Resonance frequencies in *x*-, *y*-, and *z*-axes drive are set to be 41, 42, and 175 Hz, respectively. The specification of this actuator is shown in Table 1.

When a sectional view of the actuator in *x*-*z* plane is focused, the magnetic structure is similar to those of four-pole three-phase permanent magnet synchronous motors. Therefore, this actuator is operated by vector control. The mover is driven in *x* and *z* axes independently when the field current element I_{dx} and the torque current element I_{qx} are assigned as the *z*- and *x*-axes thrust elements, respectively.

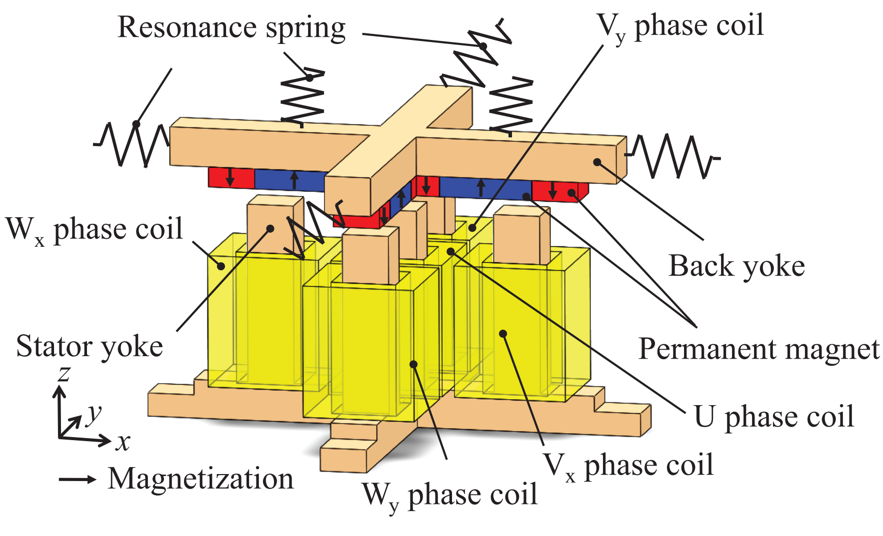

Fig. 1. Basic structure of three-DOF resonant actuator

Received: 30.06.2018. Revised: 30.06.2018. Accepted: 01.10.2018.
Transportation Systems and Technology. 2018;4(3):90-101

doi: 10.17816/transsyst20184390-101

Table 1. Specification of three-DOF resonant actuator

Parameter	**Value**		
	x-axis	**y-axis**	**z-axis**
Mass of mover [g]	214.89	55.38	21.22
Spring constant [N/mm]	14.89	3.22	29.15
Viscous damping coefficient [Ns/m]	0.997	0.44	0.528
Dimensions [mm]	31 x 31 x 18.8		
Remanence of magnet [T]	1.4		
Coil resistance [Ω]	0.24		

Because of the symmetry of magnetic circuits in x- and y-direction, the mover is also independently driven in y and z axes when the I_{dy} and I_{qy} are assigned as the z- and y-axes thrust elements, respectively. This actuator is a non-salient pole type and the thrust equation under the vector control is given as follow:

$$\begin{bmatrix} F_z & F_x & F_y \end{bmatrix}^T = \varphi \begin{bmatrix} I_{dx} + I_{dy} & I_{qx} & I_{qy} \end{bmatrix}^T \tag{1}$$

where F_x, F_y, and F_z are the thrust of the x-, y-, and z-axes, respectively, and φ is the armature interlinkage flux from the permanent magnet. A phase angle of each axis between the stator and the mover is given as follow:

$$\theta_j = \frac{j}{l}\pi \tag{2}$$

where l is the distance between north and south poles, and j is the axis of the mover. From the equations (1) and (2), the current of each phase is determined by the inverse d-q transformation, as follow:

$$\begin{bmatrix} I_U \\ I_{V_j} \\ I_{W_j} \end{bmatrix} = \sqrt{\frac{2}{3}} \begin{bmatrix} \cos\theta_j & -\sin\theta_j \\ \cos(\theta_j - 2/3\pi) & -\sin(\theta_j - 2/3\pi) \\ \cos(\theta_j + 2/3\pi) & -\sin(\theta_j + 2/3\pi) \end{bmatrix} \begin{bmatrix} I_{dj} \\ I_{qj} \end{bmatrix} \tag{3}$$

where I_U is the current of U phase coil, and I_{Vj} and I_{Wj} are the current of V_j and W_j ($j = x, y$) phase coils, respectively.

Received: 30.06.2018. Revised: 30.06.2018. Accepted: 01.10.2018.

doi: 10.17816/transsyst20184390-101

EVALUATION OF THRUST INTERFERENCE

In this chapter, thrust interference is evaluated by electromagnetic field analysis using 3-D finite element method (FEM). Fig. 2 shows the FEM model except air region. The number of tetrahedron elements and edges are approximately 1,554 000 and 1,799 000, respectively. CPU time per one step was about 10 minutes. Fig. 3 shows the analyzed current thrust characteristics in x-direction when magnetomotive force of 45 A is applied to each excitation coil (U, V_x, W_x, V_y, and W_y phase). Out of five thrust waveforms, the waveforms in the U, V_x, and W_x phase coils are sinusoidal and the phase differences of these waveforms are approximately 120 degrees in electrical angle. This result means that the actuator is able to operate in the x-axis if the three coils are excited on the basis of normal vector control theory. Fig. 4 shows the analyzed current thrust characteristics in z-direction. Thrust waveforms of U, V_x, and W_x phase coils are also sinusoidal as thrust waveforms in x-direction mentioned above.

Next, the mutual thrust interference is evaluated when the vector control which is described at the previous section is employed. Fig. 5, 6 show the static thrust characteristics when only one target current is set. In Fig. 5, the x-axis thrust is almost constant with respect to the displacement in the x- and y-directions. However, the undesirable thrust in the z-axis is generated though d-axis targets d_x and d_y are zero, respectively. This is because the thrust characteristics of U, V_x, and W_x phase coils are not complete sine wave due to the end effect. Similarly in Fig. 6, the z-axis thrust is almost constant with respect to the displacement in x- and y-directions and the undesirable x-axis thrust is slightly generated. From these

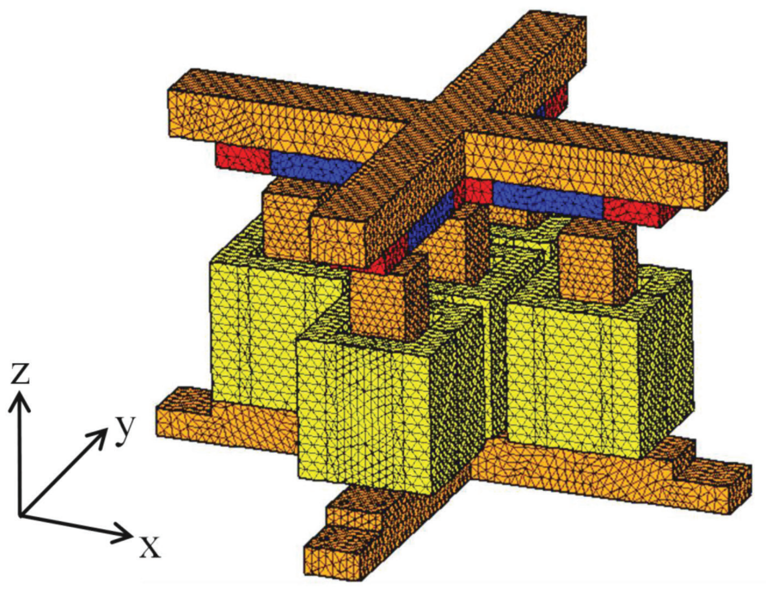

Fig. 2. FEM model

Received: 30.06.2018. Revised: 30.06.2018. Accepted: 01.10.2018.
Transportation Systems and Technology. 2018;4(3):90-101

doi: 10.17816/transsyst20184390-101

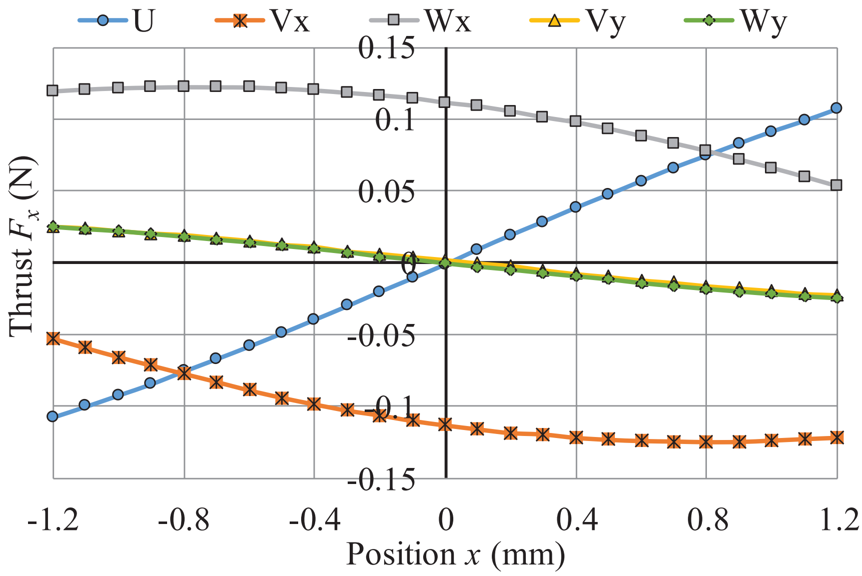

Fig. 3. Current thrust characteristic (x-axis)

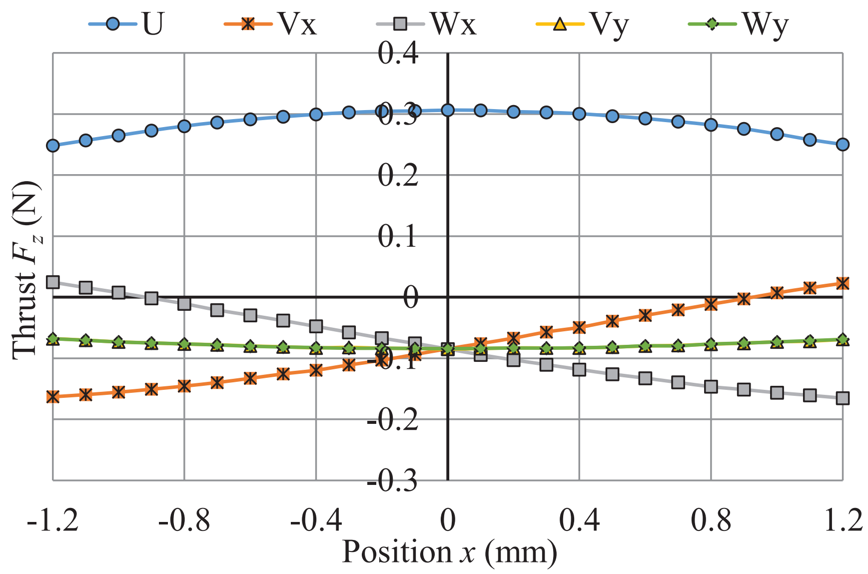

Fig. 4. Current thrust characteristic (z-axis)

results, the mutual thrust interference is tiny when the target direction of thrust is single.

Fig. 7 shows the static thrust characteristics when two target currents are simultaneously set. The x- and z-axes thrusts severely vary with respect to the displacement in the x- and y-directions. This is because V_y and W_y phase coils, which are originally used for y-axis operation, generate the thrust in the x-direction, as shown in Fig. 5. Moreover, the y-axis target current affects the z-axis thrust.

Received: 30.06.2018. Revised: 30.06.2018. Accepted: 01.10.2018.
Transportation Systems and Technology. 2018;4(3):90-101

doi: 10.17816/transsyst20184390-101

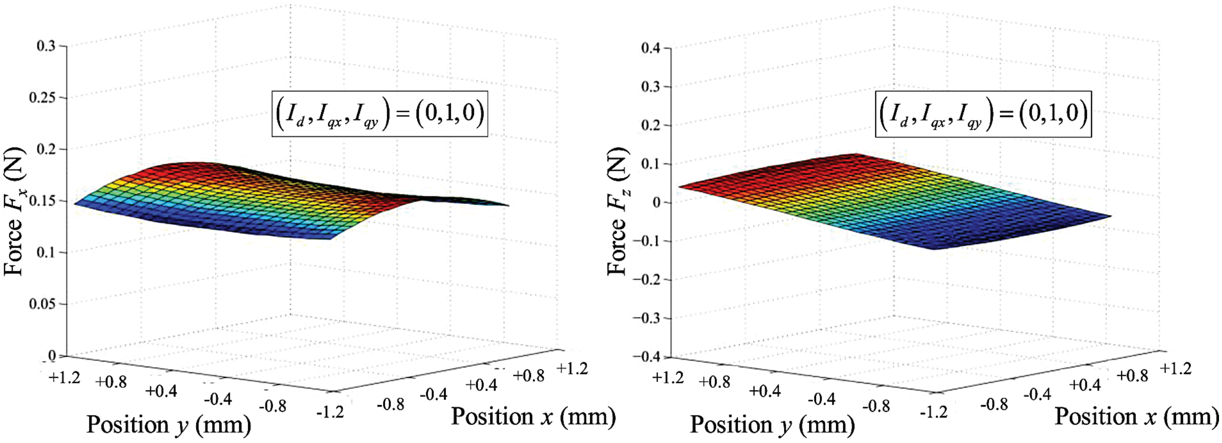

Fig. 5. Thrust characteristics under only one target current ($q_x = 1$)

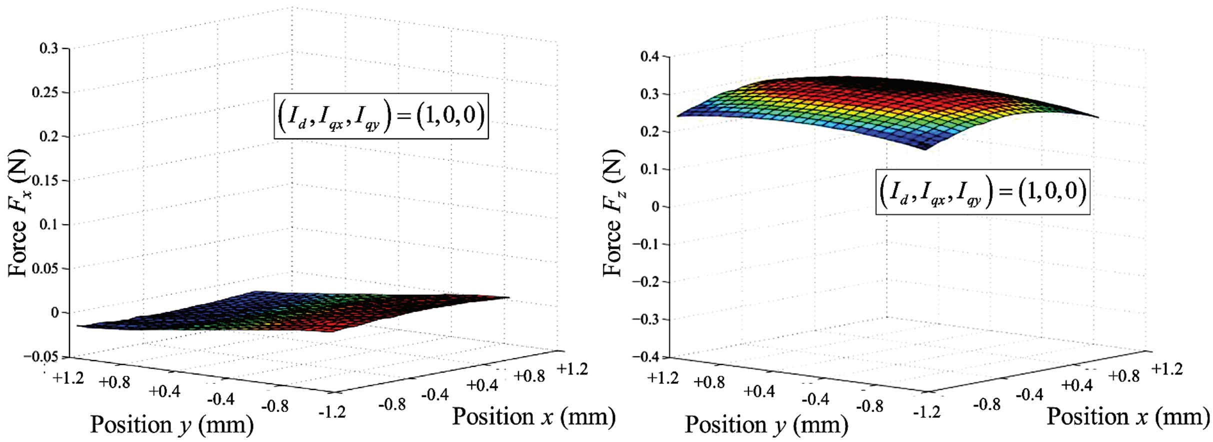

Fig. 6. Thrust characteristics under only one target current (d_x=1)

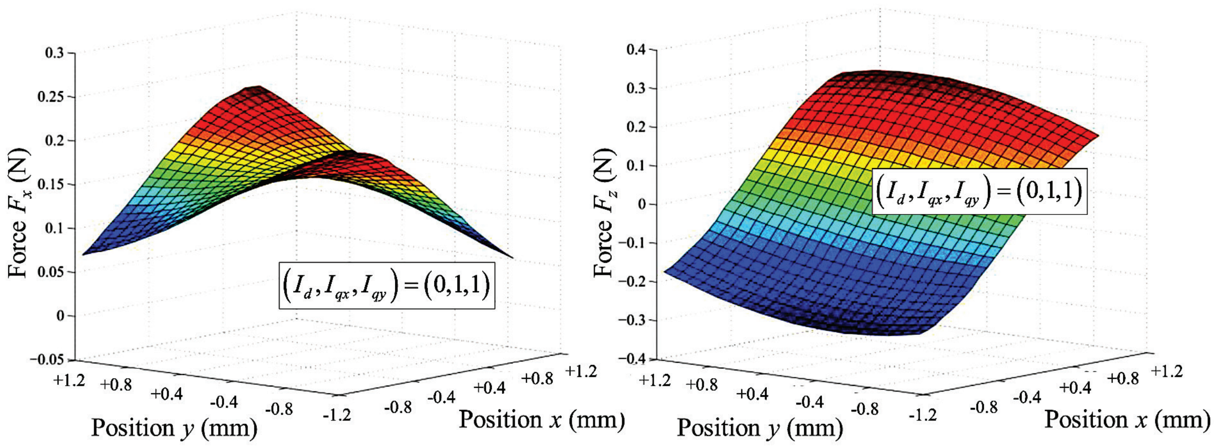

Fig. 7. Thrust characteristics under two target currents ($q_x = q_y = 1$)

Received: 30.06.2018. Revised: 30.06.2018. Accepted: 01.10.2018.
Transportation Systems and Technology. 2018;4(3):90-101

doi: 10.17816/transsyst20184390-101

Therefore, when the actuator is operated to oscillate in two or three directions, the thrust equation (3) is not suitable for obtaining a target thrust precisely.

NOVEL VECTOR CONTROL THEORY

As described in the previous chapter, the conventional vector control is not completely able to control the thrust of the actuator because U phase coil is shared. When a sectional view of the actuator in x-z plane is focused, three-phase system under the vector control corresponds to “three” actions. Two of the three are torque current (x- or y-axis drive) and field current (z-axis drive). The rest one is a condition that the sum of three-phase currents is constrained to zero. This suggests that the numbers of phases and actions are identical. On the basis of this concept, four-phase system is theoretically desirable for three-DOF resonant actuator because four-phase system corresponds to three operational actions (x-, y-, and z-axes drive) and one constraints that the sum of four-phase currents is zero.

Fig. 8 shows the schematic diagram of space vectors in the novel vector control using four-phase system. U_x, V_x and W_x phase vectors are defined in αβ plane and U_y, V_y and W_y phase vectors are defined in αγ plane. These six vectors are integrated in the αβγ space. However, U_x and U_y phase vectors are arranged in order to cancel each other. As a result, four phase vectors are defined in the αβγ space. Since αβ plane are orthogonal to αγ plane, the four phase vectors work as basis vectors of the proposed control.

Next, we form a novel dq transformation matrix. The transformation matrix from a four-phase stationary reference frame to a three-axis orthogonal stationary reference frame is represented by the following equation which contains three unknowns:

$$\begin{bmatrix} I_\alpha \\ I_\beta \\ I_\gamma \\ I_0 \end{bmatrix} = k \begin{bmatrix} \cos\theta_{un} & \cos\theta_{un} & -\cos\theta_{un} & -\cos\theta_{un} \\ \sin\theta_{un} & -\sin\theta_{un} & 0 & 0 \\ 0 & 0 & \sin\theta_{un} & -\sin\theta_{un} \\ a & a & a & a \end{bmatrix} \begin{bmatrix} I_{\mathrm{V}_x} \\ I_{\mathrm{W}_x} \\ I_{\mathrm{V}_y} \\ I_{\mathrm{W}_y} \end{bmatrix} = \left[{}^{\alpha\beta\gamma}\mathbf{C}_{\mathrm{VWVW}} \right] \begin{bmatrix} I_{\mathrm{V}_x} \\ I_{\mathrm{W}_x} \\ I_{\mathrm{V}_y} \\ I_{\mathrm{W}_y} \end{bmatrix} \tag{4}$$

Received: 30.06.2018. Revised: 30.06.2018. Accepted: 01.10.2018.

doi: 10.17816/transsyst20184390-101

where, I_α, I_β, and I_γ are the αβγ orthogonal reference frame quantities, I_0 is the zero sequence current, I_{vx}, I_{wx}, I_{vy}, and I_{wy} are the four-phase stationary reference frame quantities. θ_{un} is the unknown angle between the α-axis and W_x phase vector. The unknown coefficients a and k are required to satisfy power invariance before and after the transformation. In order to satisfy it, the product of the matrix $[{}^{\alpha\beta\gamma}\boldsymbol{C}_{\mathrm{VWVW}}]$ and its transpose matrix $[{}^{\mathrm{VWVW}}\boldsymbol{C}_{\alpha\beta\gamma}]$ needs to be identity matrix. Therefore, the following equation is obtained and three unknown values are identified:

$$\left[{}^{\alpha\beta\gamma}\mathbf{C}_{\mathrm{VWVW}}\right]\left[{}^{\alpha\beta\gamma}\mathbf{C}_{\mathrm{VWVW}}\right]^T = k^2\begin{bmatrix} 4\cos^2\theta_{un} & 0 & 0 & 0 \\ 0 & 2\sin^2\theta_{un} & 0 & 0 \\ 0 & 0 & 2\sin^2\theta_{un} & 0 \\ 0 & 0 & 0 & 4a^2 \end{bmatrix} = \\ = [\mathbf{I}] \begin{cases} \theta_{un} \cong 125\,\mathrm{deg.} \Leftrightarrow \cos\theta_{un} = -\dfrac{1}{\sqrt{3}} \\ k = \dfrac{\sqrt{3}}{2} \\ a = \dfrac{1}{\sqrt{3}} \end{cases} \qquad (5)$$

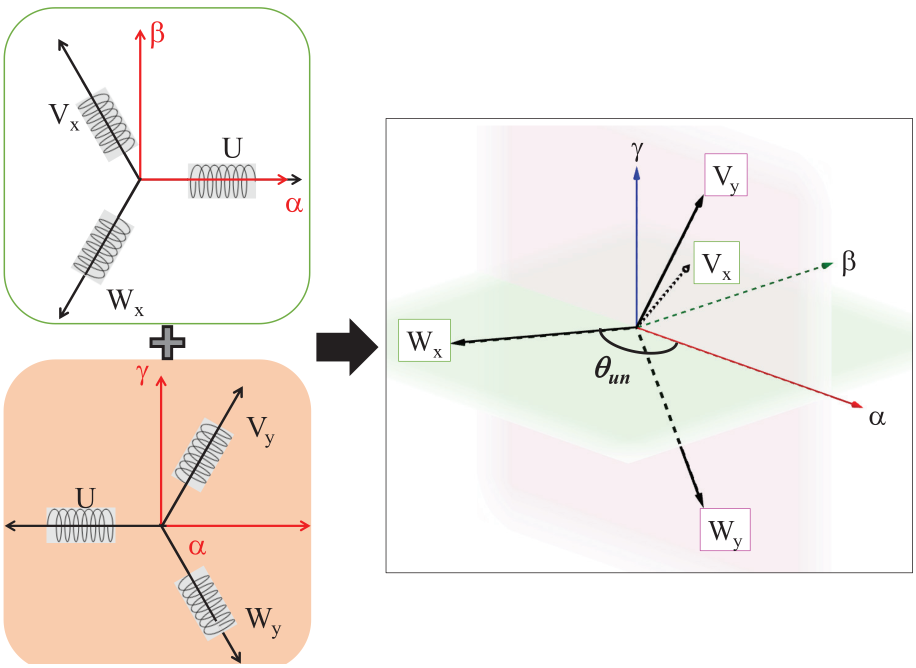

Fig. 8. Schematic diagram of novel vector control theory

Received: 30.06.2018. Revised: 30.06.2018. Accepted: 01.10.2018.
Transportation Systems and Technology. 2018;4(3):90-101

doi: 10.17816/transsyst20184390-101

This result suggests that the four-phase system has a slightly different angle (125 deg.) from that of the normal three-phase system (120 deg.). Next, dq transformation for three-DOF resonant actuator is introduced. The proposed vector control employs Euler angles representaion in order to express the two electrical angles θ_x and θ_y. Fig. 9 shows the schematic diagram of dq transformation by Euler angles. The αβγ reference frame is converted to α'β'γ reference frame by rotating around β-axis by θ_y, as shown in Fig. 9b. After that, The α'β'γ reference frame is converted to d-q_x-q_y rotational reference frame by rotating around γ'-axis by θ_x, as shown in Fig. 9c. The transformation matrix from a three-axis stationary reference frame to a three-axis rotational reference frame is expressed by the following equation.

$$\begin{bmatrix} I_{\mathrm{d}} \\ I_{\mathrm{q}_x} \\ I_{\mathrm{q}_y} \\ I_0 \end{bmatrix} = \begin{bmatrix} \cos\theta_x \cos\theta_y & \sin\theta_x & \cos\theta_x \sin\theta_y & 0 \\ -\sin\theta_x \cos\theta_y & \cos\theta_x & -\sin\theta_x \sin\theta_y & 0 \\ -\sin\theta_y & 0 & \cos\theta_y & 0 \\ 0 & 0 & 0 & 1 \end{bmatrix} \begin{bmatrix} I_\alpha \\ I_\beta \\ I_\gamma \\ I_0 \end{bmatrix} = \left[{}^{\mathrm{dq}}\mathbf{C}_{\alpha\beta\gamma} \right] \begin{bmatrix} I_\alpha \\ I_\beta \\ I_\gamma \\ I_0 \end{bmatrix} \quad (6)$$

From equations (5) and (6), The dq transformation matrix is obtained:

$$\begin{bmatrix} I_d \\ I_{q_x} \\ I_{q_y} \end{bmatrix} = \frac{\sqrt{3}}{2} \times \begin{bmatrix} c\theta_x c\theta_y c\theta_{un} + s\theta_x s\theta_{un} & c\theta_x c\theta_y c\theta_{un} - s\theta_x s\theta_{un} & -c\theta_x c(\theta_y + \theta_{un}) & -c\theta_x c(\theta_y + \theta_{un}) \\ -s\theta_x c\theta_y c\theta_{un} + c\theta_x s\theta_{un} & -s\theta_x c\theta_y c\theta_{un} - c\theta_x s\theta_{un} & s\theta_x c(\theta_y + \theta_{un}) & s\theta_x c(\theta_y - \theta_{un}) \\ -s\theta_y s\theta_{un} & -s\theta_y s\theta_{un} & s(\theta_y + \theta_{un}) & s(\theta_y + \theta_{un}) \end{bmatrix} \times \begin{bmatrix} I_{V_x} \\ I_{W_x} \\ I_{V_y} \\ I_{W_y} \end{bmatrix}, \quad (7)$$

where, s and c are the abbreviations for sine and cosine, respectively.

Received: 30.06.2018. Revised: 30.06.2018. Accepted: 01.10.2018.

Transportation Systems and Technology. 2018;4(3):90-101
doi: 10.17816/transsyst20184390-101

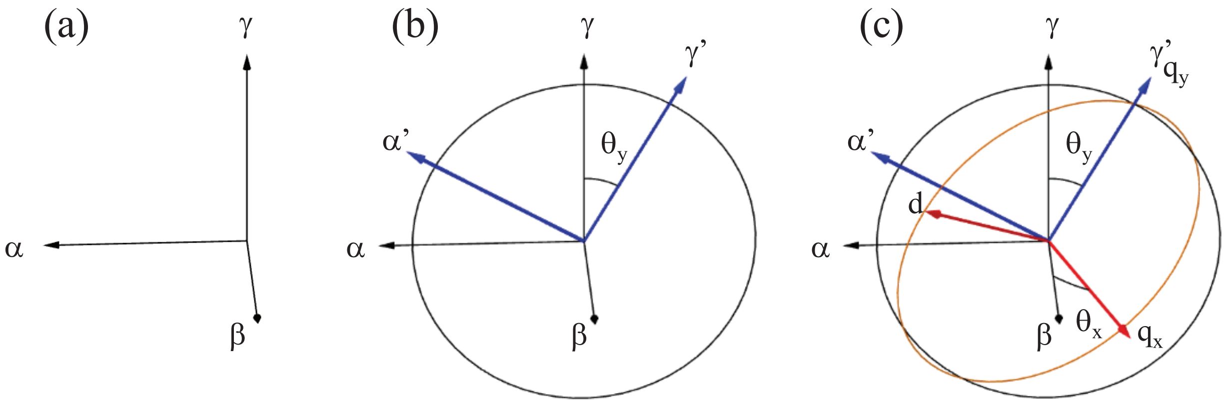

Fig. 9. 3-D dq transformation by Euler angles representation

PERFORMANCE COMPARISON

The proposed vector control theory is applied to the three-DOF resonant actuator in order to confirm its effectiveness. Fig. 10 shows the static thrust characteristics when only one target current is set under the proposed control. In this case, the *x*-axis thrust is almost constant with respect to *x*- and *y*-axes displacements and this result is the same as that shown in Fig. 5. Similarly, the *z*-axis thrust is almost zero because the target current I_d equals zero. Fig. 11 shows the static thrust characteristics when two target currents are set simultaneously under the proposed control. It can be seen from the comparison between Fig. 11, 7 that the proposed vector control is able to decrease the thrust interferences from the other target current.

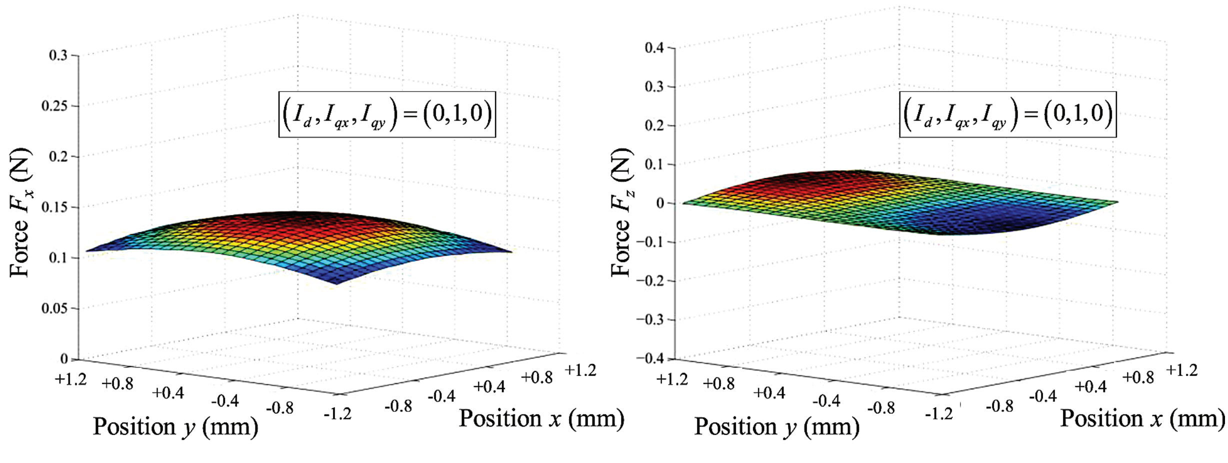

Fig. 10. Thrust characteristics under the proposed vector control ($q_x = 1$)

Received: 30.06.2018. Revised: 30.06.2018. Accepted: 01.10.2018.
Transportation Systems and Technology. 2018;4(3):90-101

doi: 10.17816/transsyst20184390-101

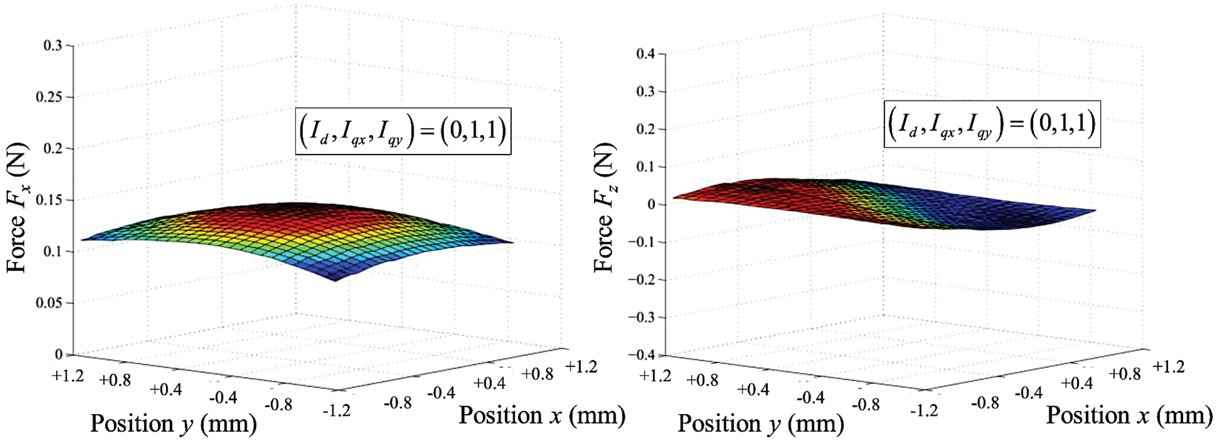

Fig. 11. Thrust characteristics under the proposed vector control (q_x=q_y=1)

CONCLUSION

In this paper, we propose a novel vector control theory to improve a controllability of our three-DOF resonant actuator. The proposed control have an originality in that a four-phase system was used, not a combination of two sets of three-phase system. A dq transformation matrix for this actuator was successfully derived on the basis of a new phase angle (125 deg.) and 3-D rotation by Euler angles representation. As a result, the proposed control decreased the thrust interference from the other target current and its effectiveness was validated.

There are already several studies dealing with d-q transformation theory of multiphase induction motors [12, 13]. However, we were not able to confirm any studies for multi-DOF electromagnetic actuators. Moreover, the proposed method have a great potential to apply to a two-DOF spherical actuator [14] because its magnet arrangement is similar to that of the three-DOF resonant actuator.

REFERENCES

1. Hirata K, Yamamoto T, Yamaguchi T, Kawase Y, Hasegawa Y. Dynamic analysis method of two-dimensinal linear oscillatory actuator employing finite element method. *IEEE Trans. Magn.* 2007;43(4):1441-1444. doi: 10.1109/tmag.2007.891407
2. Jang SM, Choi JY, Jeong SS. Electromagnetic analysis and control parameter estimation of moving-coil linear oscillatory actuator. *Journal of Applied Physics*. 2006; 99, 08R307. doi: 10.1063/1.2165606
3. Lee H, Moon H, Wang S, Park K. Iron loss analysis of linear oscillating actuator for linear compressor. *International Journal for Computation and Mathematics in Electrical and Electronic Engineering*. 2006;25(2):487-495. doi: 10.1108/03321640610649140
4. Utsuno M, Takai M, Mizuno T, Yamada H. Comparison of the losses of a moving-magnet type linear oscillatory actuator under two driving methods. *IEEE Trans. Magn.* 2002;38(5):3300-3302. doi: 10.1109/tmag.2002.802291

Received: 30.06.2018. Revised: 30.06.2018. Accepted: 01.10.2018.
Transportation Systems and Technology. 2018;4(3):90-101

doi: 10.17816/transsyst20184390-101

5. Zhu ZQ, Chen X, Howe D, Iwasaki S. Electromagnetic modeling of a novel linear oscillating actuator. *IEEE Trans. Magn.* 2008;44(11):3855-3858. doi: 10.1109/tmag.2008.2001323
6. Yamaguchi T, Kawase Y, Sato K, Suzuki S, Hirata K, Ota T, Hasegawa Y. Trajectory analysis of 2-D magnetic resonant actuator. *IEEE Trans. Magn.* 2009;45(3):1732-1735. doi: 10.1109/tmag.2009.2012800
7. Suzuki S, Kawase Y, Yamaguchi T, Shibayama Y, Hirata K, Ota T. 3-D finite element analysis of dynamic characteristics of spherical resonant actuator. *Proc. of International Conference on Electrical Machines*. 2010; Roma, Italy. doi: 10.1109/icelmach.2010.5608213
8. Yoshimoto T, Asai Y, Hirata K, Ota T. Dynamic characteristics of novel two-DOF resonant actuator by vector control. *IEEE Trans. Magn.* 2012;48(11):2985-2988. doi: 10.1109/tmag.2012.2198203
9. Yoshimoto T, Asai Y, Hirata K, Ota, T. Simplified position estimation using back-EMF for two-DOF linear resonant actuator. *IEEE Trans. Magn.* 2014;50(2):7023804. doi: 10.1109/tmag.2013.2282496
10. Yoshimoto T, Asai Y, Hirata K, Ota T. Dynamic characteristic analysis and experimental verification of 2-DoF resonant actuator under feedback control. *Journal of the Japan Society of Applied Electromagnetics and Mechanics*. 2015;23(3):521-526. doi: 10.14243/jsaem.23.521
11. Kato M, Hirata K, Fujita K. Dynamic Characteristics of Three-Degree-of-Freedom Resonant Actuator. *International Journal for Computation and Mathematics in Electrical and Electronic Engineering*. 2018;37(6): to be published.
12. Leila P, Hamid T. Five-Phase Permanent-Magnet Motor Drives. *IEEE Trans. Ind. Appl.* 2005;41(1):30-37. doi: 10.1109/tia.2004.841021
13. Emil L. Multiphase Electric Machines for Variable-Speed Applications. *IEEE. Trans. Ind. Electron.* 2008;55(5):1893-1909. doi: 10.1109/tie.2008.918488
14. Tsukano M, Sakaidani Y, Hirata K, Niguchi N, Maeda S, Zaini A. Analysis of 2-Degree of Freedom Outer Rotor Spherical Actuator Employing 3-D Finite Element Method. *IEEE Trans. Magn.* 2013;49(5):2233-2236. doi: 10.1109/tmag.2012.2237390

Information about the authors:
Kato Masayuki, Master of Engineering, Doctor-course Student;
Yamadaoka 2-1, Suita-shi, Osaka-fu, Japan, 5650871
ORCID: 0000-0002-0856-1588;
E-mail: masayuki.kato@ams.eng.osaka-u.ac.jp

Hirata Katsuhiro, Doctor of Engineering, Professor;
ORCID: 0000-0002-5597-5265;
E-mail: k-hirata@ams.eng.osaka-u.ac.jp

To cite this article:
Kato M, Hirata K. Control of Three-Degree-of-Freedom Resonant Actuator Driven by Novel Vector Control. *Transportation Systems and Technology.* 2018;4(3):90-101. doi: 10.17816/transsyst20184390-101